Supplementary Information (SI) for Journal of Materials Chemistry B.

Electronic Supporting Information

Combat Food Spoilage by Tackling Drug Resistance: Sulfur-Doped Carbon Nanozymes as Effective Tomato Coatings

Evans Okoffuo Asare[1]†, Enrico Benassi[2]*†, Tri Pham[3]*, Enrico Marsili[4], and Haiyan Fan[1]*

[1] *Department of Chemistry, School of Sciences and Humanities, Nazarbayev University, Astana, Kazakhstan.*
[2] *Infochemistry Scientific Center, ITMO University, Saint-Petersburg 191002, Russian Federation.*
[3] *Department of Biology, School of Sciences and Humanities, Nazarbayev University, Astana, Kazakhstan*
[4] *University of Nottingham Ningbo, Faculty of Science and Engineering, China.*

† These authors equally contributed.
* Corresponding author's e-mail address: ebenassi3@gmail.com, tri.pharm@nu.edu.kz, haiyan.fan@nu.edu.kz

Table S1. Shows the percentage CHNS elemental composition of the synthesized Cys-MR NPs and NAC-MR NPs.

Sample	Elemental Composition			
	N [%]	**C [%]**	**H [%]**	**S [%]**
Cys-MR NPs	22.04±0.1	39.98±0.6	9.62±0.1	8.35±0.3
NAC-MR NPs	20.78±1.5	39.47±1.7	7.93±0.6	7.97±0.7

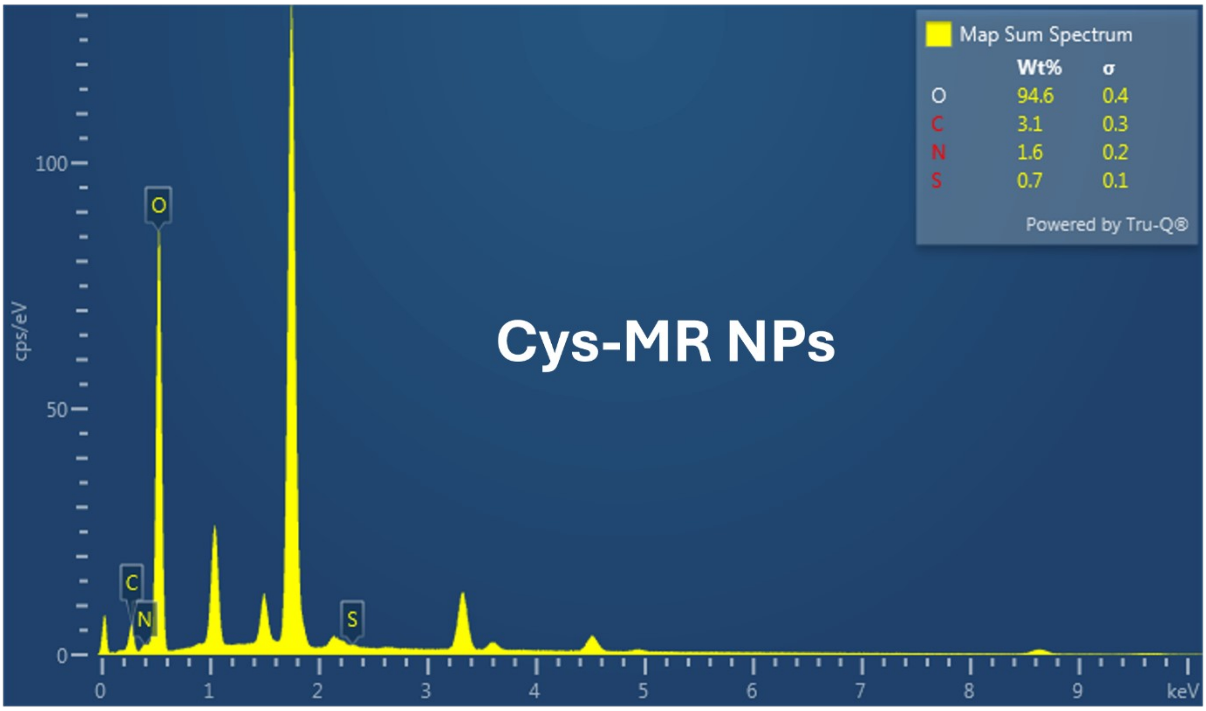

Figure S1. EDX spectra of Cys-MR NPs. EDX spectra was obtained with SEM Crossbeam 540 and processed with oxford instrument nanoanalyzer detector.

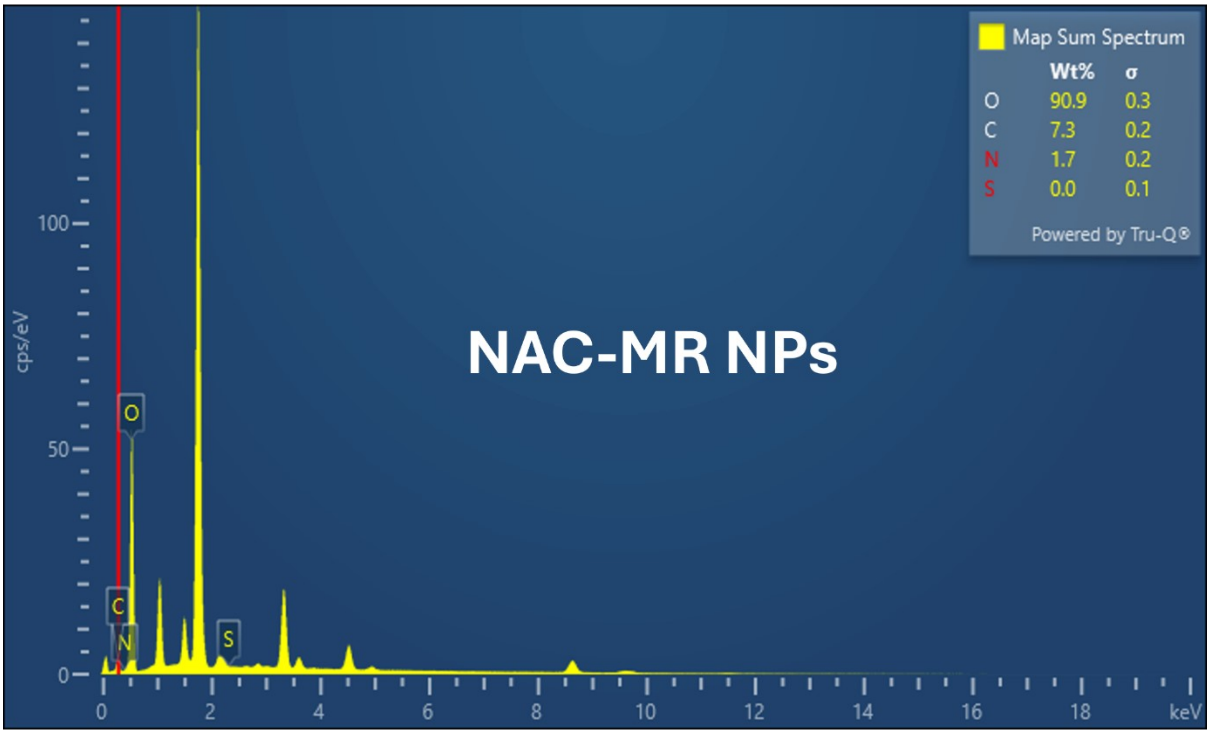

Figure S2. EDX spectra of NAC-MR NPs. EDX spectra was obtained with SEM Crossbeam 540 and processed with oxford instrument nanoanalyzer detector.

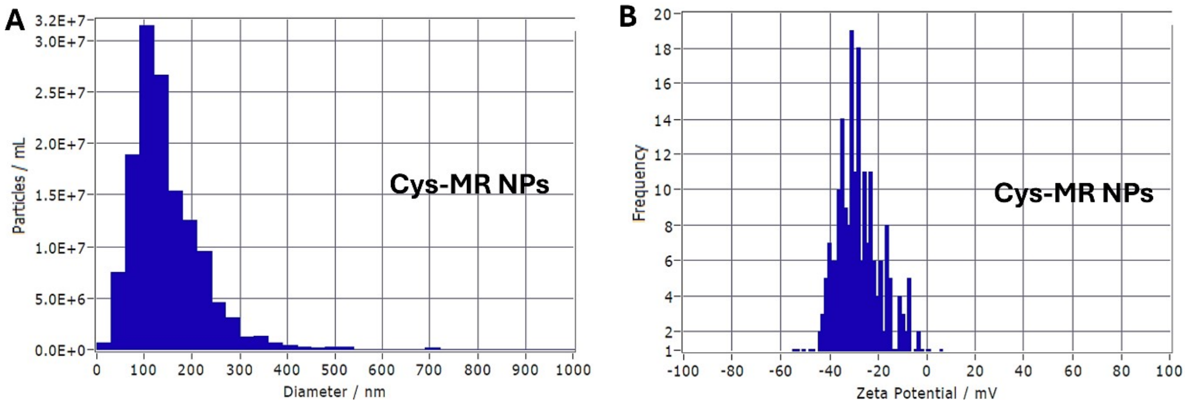

Figure S3. DLS size and ELS zeta potential distribution of Cys-MR NPs.

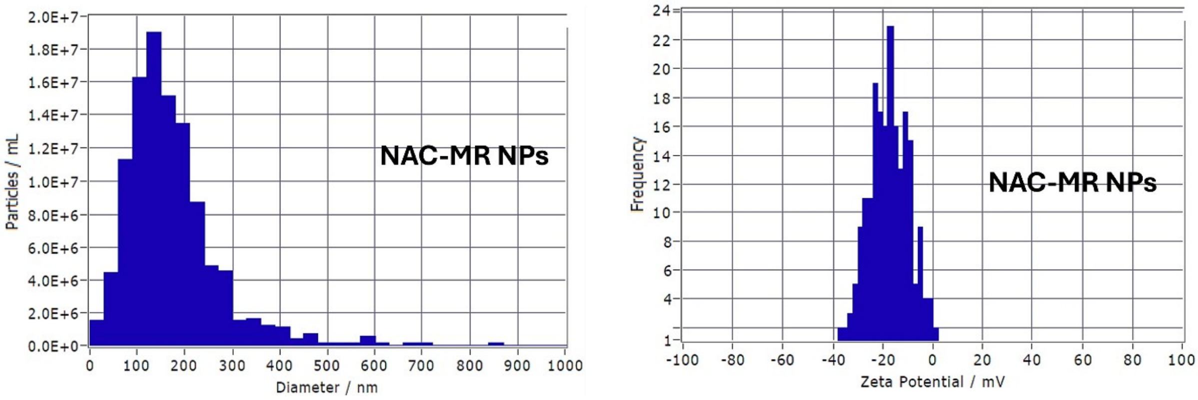

Figure S3. DLS size and ELS zeta distribution of NAC-MR NPs.

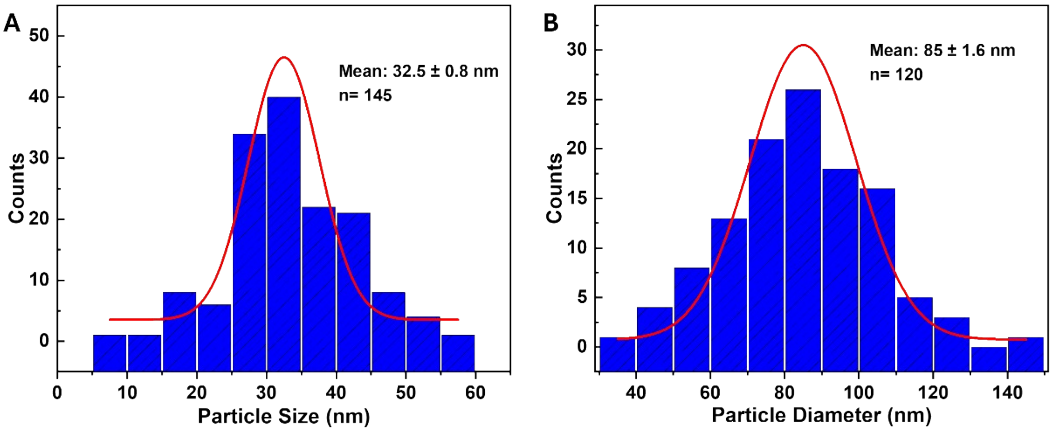

Figure S4. (A) Cys-MR NPs and (B) NAC-MR NPs size distribution obtained from SEM imaging.

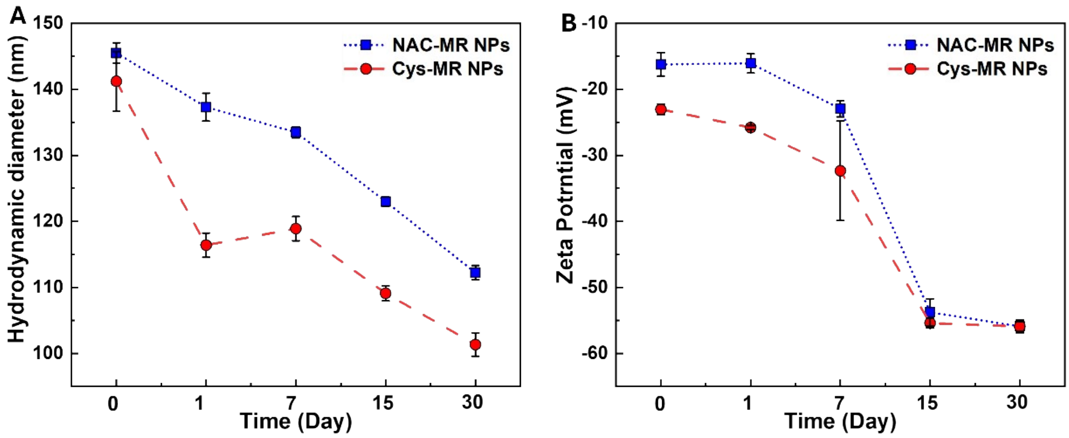

Figure S5. Colloidal stability of Cys-MR NPs and NAC-MR NP within a period of 30 days. (A) DLS mean hydrodynamic diameter measured at pH 7.5 within 30 days. (B) ELS mean zeta potential measured at pH 7.5 and 25 °C within 30 days.

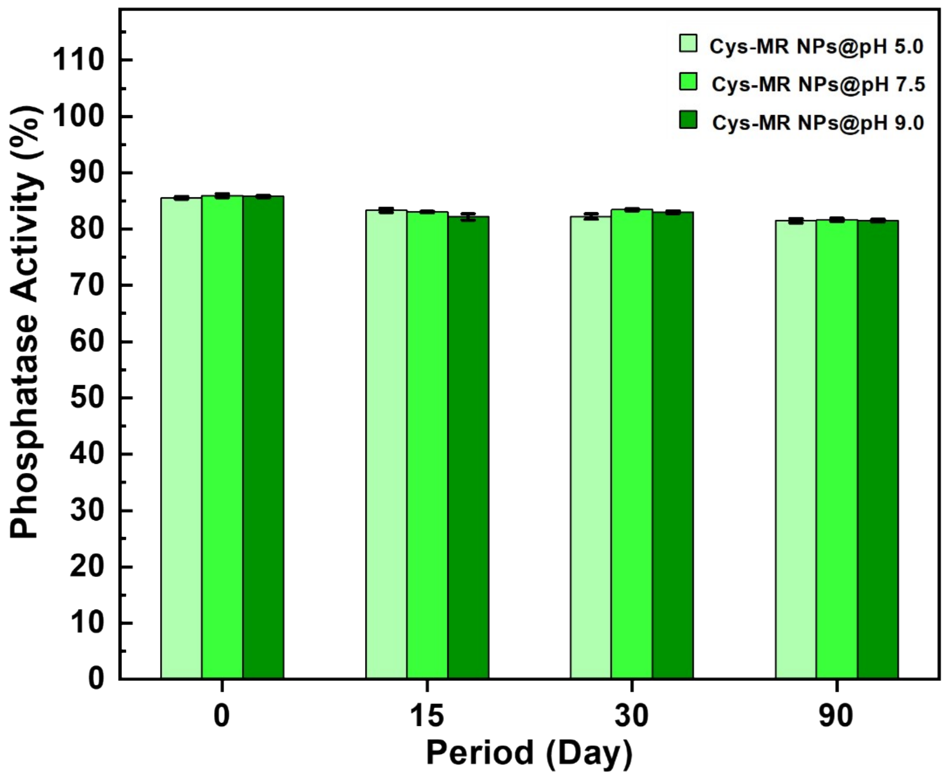

Figure S6. Compared Phosphatase activity of Cys-NPs at various pH within 90 days. Each data indicates the average and error bars indicate ±SD for trice trials (N=3, ±SD).

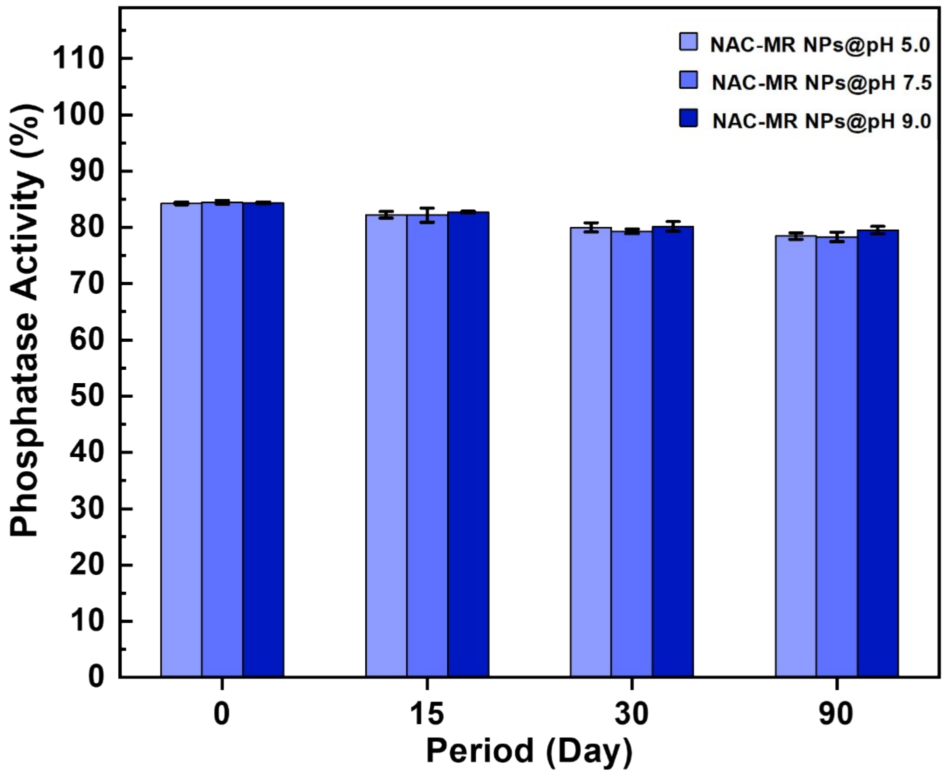

Figure S7. Compared Phosphatase activity of NAC-NPs at various pH within 90 days. Each data indicates the average and error bars indicate ±SD for trice trials (N=3, ±SD).

Table S2. Shows the comparative Michaelis-Menten mechanistic kinetic reaction of various enzymes with BCIP/NBT substrate.

Enzymes	V_{max} / μM min^{-1}	K_m / mM	Reference
Calf-intestinal ALP	6.38 ± 0.51	0.56 ± 0.15	[36]
SN-CNPs	20.82 ± 1.36	0.21 ± 0.01	[36]
Cys-MR NPs	10.70 ± 1.00	0.12 ± 0.05	This work
NAC-MR NPs	10.10 ± 1.00	0.15 ± 0.03	This work

Cys-MR NPs

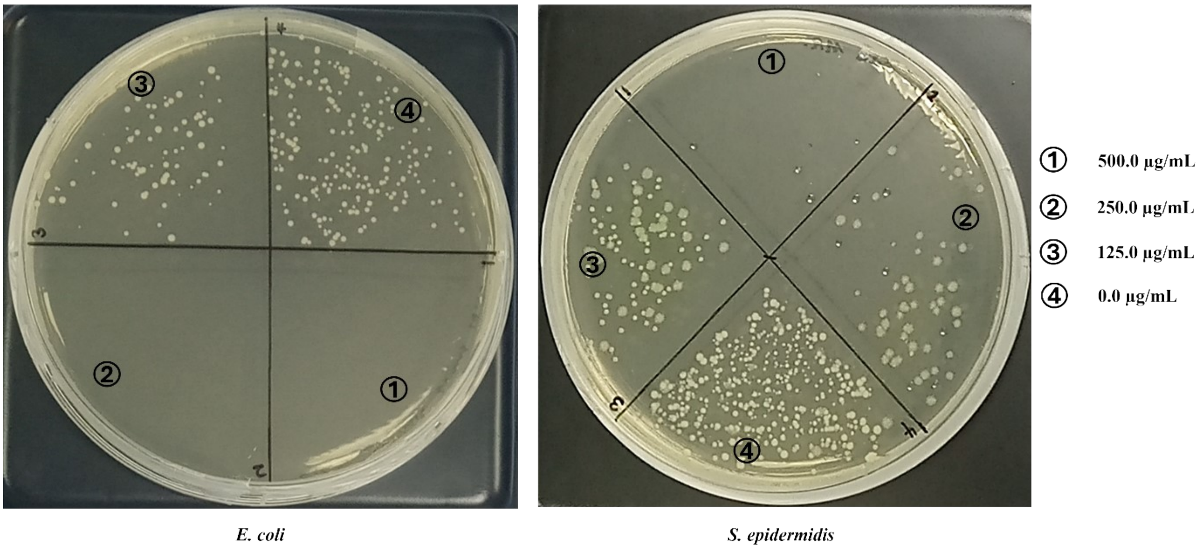

Figure S8. Colonies of bacterial strains formed on nutrient agar (NA) after 18 h incubation after exposure with Cys-MR NPs.

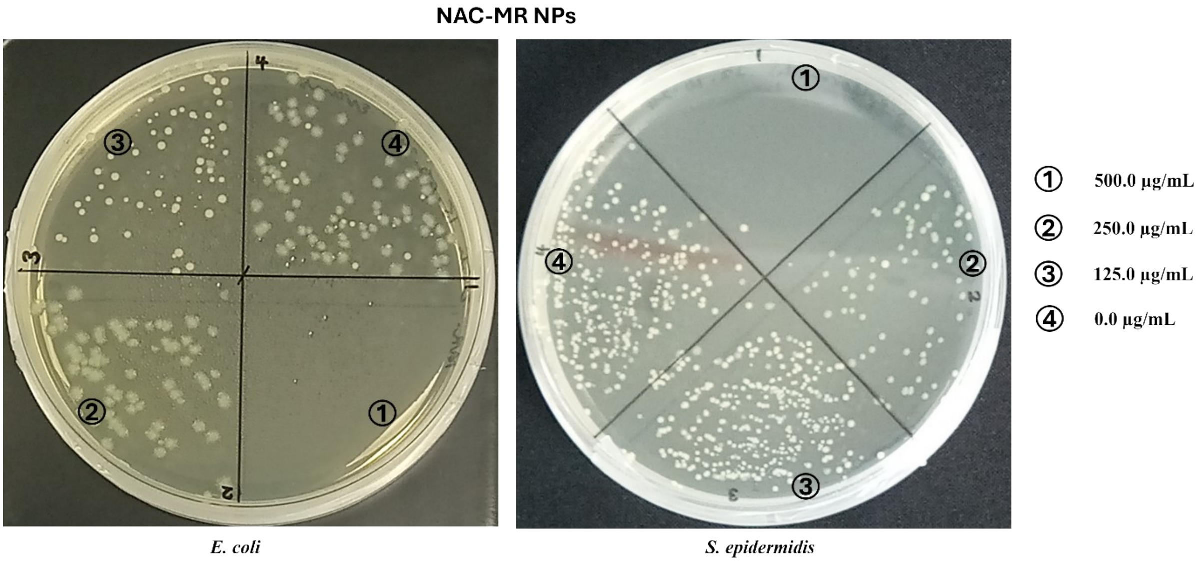

Figure S9. Colonies of bacterial strains formed on nutrient agar (NA) after 18 h incubation after exposure with NAC-MR NPs.

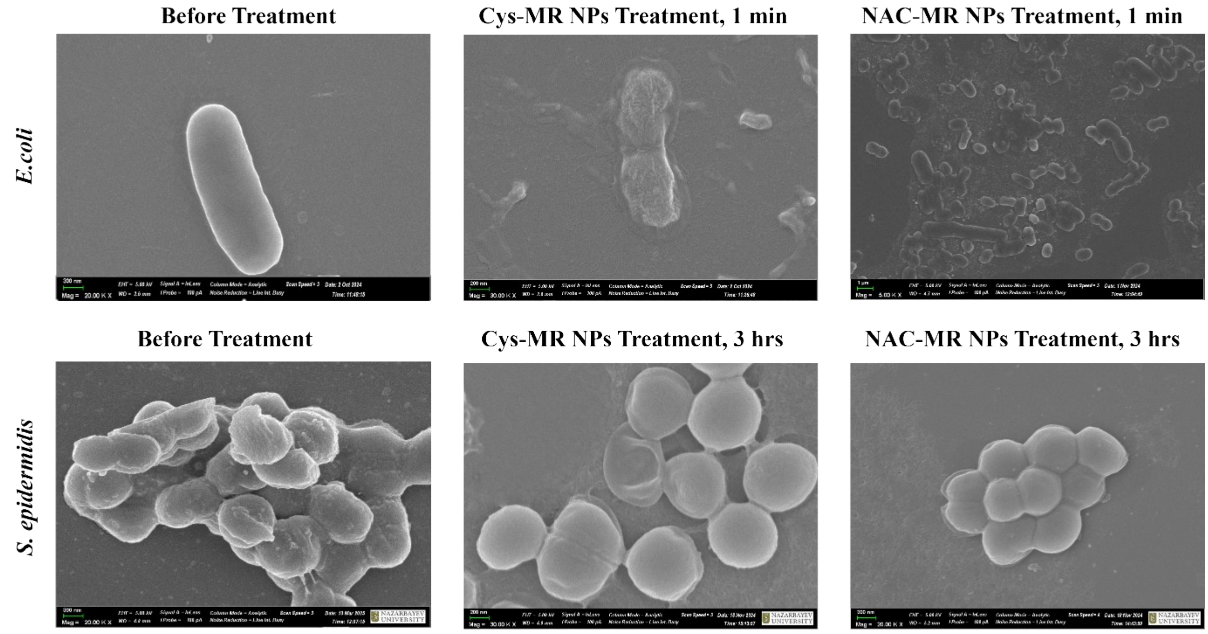

Figure S10. SEM images of the bacterial strains before and after treatment with NAC-MR NPs over a range of incubation periods. SEM ZEISS Crossbeam 540 was used for imaging at 123v, 361kx magnification and 4s exposure.

$$OD = \frac{X_m}{1 + exp\left\{2\left[1 - 2\frac{V_m}{X_m}(t - \lambda)\right]\right\}} \quad (1)$$

Table S3. Parameters upon nonlinear fitting of the bactericidal kinetics against *E. coli* and *S. epidermidis*.

		[Cys-MR NPs] / ($\mu g/mL$)	V_m / (OD/h)	X_m	λ / h	adj.-R^2
Cys-MR	E. coli	15.6	0.162 $\pm$ 0.012	0.99 $\pm$ 0.03	2.32 $\pm$ 0.19	0.991
		31.3	0.160 $\pm$ 0.004	1.04 $\pm$ 0.01	2.16 $\pm$ 0.09	0.999
		62.5	0.174 $\pm$ 0.012	1.02 $\pm$ 0.01	2.58 $\pm$ 0.14	0.998
		125	0.155 $\pm$ 0.008	0.94 $\pm$ 0.04	3.27 $\pm$ 0.13	0.990
		250	0.014 $\pm$ 0.002	0.10 $\pm$ 0.01	10.20 $\pm$ 0.68	0.971
	S. epi	62.5	0.164 $\pm$ 0.013	0.92 $\pm$ 0.05	2.23 $\pm$ 0.16	0.976
		125	0.157 $\pm$ 0.011	0.85 $\pm$ 0.03	3.46 $\pm$ 0.14	0.990
		250	0.008 $\pm$ 0.000	0.09 $\pm$ 0.00	6.81 $\pm$ 0.51	0.999

		[NAC-MR NPs] / ($\mu g/mL$)	V_m / (OD/h)	X_m	λ / h	adj.-R^2
NAC-MR	E. coli	15.6	0.162 $\pm$ 0.012	0.99 $\pm$ 0.03	2.24 $\pm$ 0.20	0.992
		31.3	0.150 $\pm$ 0.011	1.03 $\pm$ 0.03	2.16 $\pm$ 0.09	0.999
		62.5	0.201 $\pm$ 0.021	0.97 $\pm$ 0.04	2.91 $\pm$ 0.22	0.985
		125	0.201 $\pm$ 0.021	0.97 $\pm$ 0.04	2.91 $\pm$ 0.22	0.985
		250	0.172 $\pm$ 0.016	0.87 $\pm$ 0.03	2.50 $\pm$ 0.13	0.990
	S. ep	15.6	0.320 $\pm$ 0.053	1.01 $\pm$ 0.05	2.60 $\pm$ 0.31	0.971
		31.3	0.172 $\pm$ 0.010	0.98 $\pm$ 0.02	2.41 $\pm$ 0.15	0.995
		62.5	0.224 $\pm$ 0.026	0.99 $\pm$ 0.02	3.43 $\pm$ 0.34	0.994
		125	0.198 $\pm$ 0.017	0.98 $\pm$ 0.03	2.89 $\pm$ 0.21	0.991
		250	0.142 $\pm$ 0.007	0.93 $\pm$ 0.02	2.93 $\pm$ 0.18	0.998

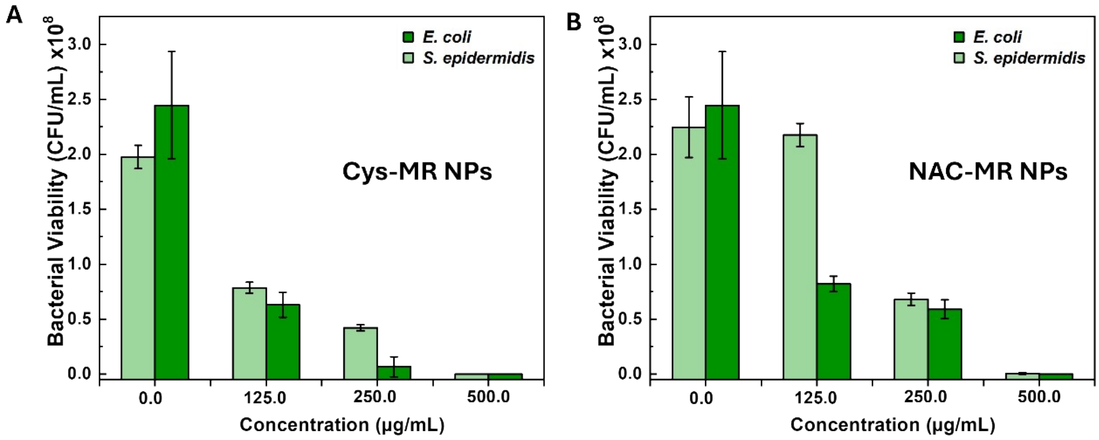

Figure S11. Bacterial viability after 24 h treatment with the Cys-MR NPs and NAC-MR NPs under 37 °C. Each data indicates the average and error bars indicate ±SD for trice trials (N=3, ±SD).

Table S4. Comparison of enzymatic parameters and antibacterial quantities among different nanozymes.

Nanozyme	MIC (µg/mL)	Substrate, Cofactor	Kinetics Parameters (Km, V_{max})	Targets	Antimicrobial Mechanism	Reference
LCDs	-	TMB, H_2O_2	11.2 mM, 1.01 $mgL^{-1} min^{-1}$	*E. coli S. aureus*	ROS generation	Ref [49]
LCDs-OA	-	TMB, H_2O_2	0.59 mM, 2.79 $mgL^{-1} min^{-1}$	*E. coli S. aureus*	ROS generation	Ref [49]
N-CNTs@Co	40 - 60	TMB, H_2O_2	Km ≈ 100.2 µM, Vmax ≈ 1.3 µM s^{-1}	*E. coli, S. aureus*	ROS generation	He etal (2021)
CNQDs	50	TMB, H_2O_2	-	*E. coli, S. aureus, B. subtilis*	·OH generation	Li et al. (2018)
o-CNTs	100	TMB, H_2O_2	-	*E. coli, S. aureus*	·OH generation	Wang et al. (2018)
NSP-CQDs	-	TMB, H_2O_2	Km ≈ 0.47 mM, Vmax ≈ 18.81µM s^{-1}	*E. coli, S. aureus*	·OH generation	Tripathi et al. (2020)
SAF NCs	62.5	TMB, H_2O_2	Km ≈ 11.95 µM, Vmax ≈ 22.3 µM s^{-1}	*E. coli, S. aureus*	·OH generation	Huo *et al.* (2019)
LCDs-OA	50	TMB, H_2O_2	Km ≈ 0.16 mM, Vmax ≈ 10.92 $\mu Mmin^{-1}$	*E. coli, MDR S. aureus*	ROS generation	Pan et al. (2024)
SN-CNPs	63, 250	BCIP/NBT	Km ≈ 0.21 mM, Vmax ≈ 20.82 $\mu Mmin^{-1}$	*E. coli, L. lactis*	Dephosphorylation	Nurtay et al. (2023)
PAA-Cnp/Ce^{3+}	50 - 75	NPPC	Km ≈ 171.8 mM, Vmax ≈ 492 μMh^{-1}	*Salmonella, E. coli, K. pneumoniae,*	Dephosphorylation	Ref [50]
Cnp	-	NPPC	Km ≈ 9.8 mM, Vmax ≈ 456 μMh^{-1}	*Salmonella, E. coli, K. pneumoniae,*	Dephosphorylation	Ref [50]

Reference

1. He, S., Huang, J., Zhang, Q., Zhao, W., Xu, Z., Zhang, W. Bamboo-like nanozyme based on nitrogen-doped carbon nanotubes encapsulating cobalt nanoparticles for wound antibacterial applications. *Adv. Funct. Mater.* 2021, 31, 41. **https://doi.org/10.1002/adfm.202105198**

2. Li, H., Huang, J., Song, Y., Zhang, M., Wang, H., Lu, F., et al. Degradable carbon dots with broad-spectrum antibacterial activity. *ACS Appl. Mater. Interfaces.* 2018, **10**, 26936–26946. https://doi.org/10.1021/acsami.8b08832

3. H. Wang , P. H. Li , D. Q. Yu , Y. Zhang , Z. Z. Wang , C. Q. Liu , H. Qiu , Z. Liu , J. S. Ren and X. G. Qu. Unraveling the Enzymatic Activity of Oxygenated Carbon Nanotubes and Their Application in the Treatment of Bacterial Infections. *Nano Lett.* 2018, **18** , 3344 —3351. https://doi.org/10.1021/acs.nanolett.7b05095

4. K. M. Tripathi , H. T. Ahn , M. Chung , X. A. Le , D. Saini , A. Bhati , S. K. Sonkar , M. I. Kim and T. Kim. N, S, and P-Co-doped Carbon Quantum Dots: Intrinsic Peroxidase Activity in a Wide pH Range and Its Antibacterial Applications. *ACS Biomater. Sci. Eng.*, 2020, **6** , 5527 —5537. https://doi.org/10.1021/acsbiomaterials.0c00831

5. M. F. Huo , L. Y. Wang , H. X. Zhang , L. L. Zhang , Y. Chen and J. L. Shi. Construction of Single-Iron-Atom Nanocatalysts for Highly Efficient Catalytic Antibiotics. *Small*, 2019, **15**, 1901834. **https://doi.org/10.1002/smll.201901834**

6. Y. Pan, D. Sun, L. Kong, Y, Liu, H. Li, D, Yu, W. Jiang, J. Zhan. Self-adaptive carbon nanozyme regulation of ROS balance for bacteria-infected wound therapy. *Chemical Engineering Journal*. 2024, **499**, 155904. https://doi.org/10.1016/j.cej.2024.155904.

7. Khulbe, K., Karmakar, K., Ghosh, S., Chandra, K., Chakravortty, 10.1021/acsabm.0c00363. D., and Mugesh, G. Nanoceria-based phospholipase-mimetic cell membrane disruptive antibiofilm agents. *ACS Appl. Bio Mater.* 2020, 3, 7, 4316–4328.

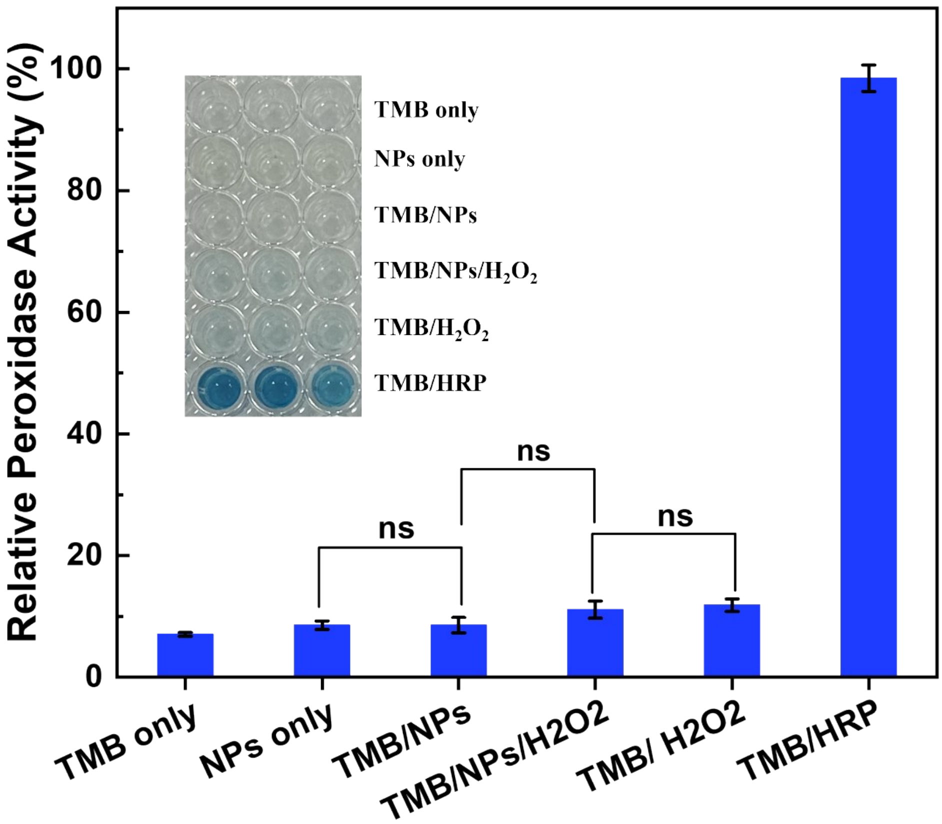

Figure S12. ROS generation capability of Cys-MR NPs. Peroxidase activity of shown by various possible TMB oxidative groups at pH 7.4 at 25 °C. Absorbance was read at 652 nm after 30 mins of allowed reaction.

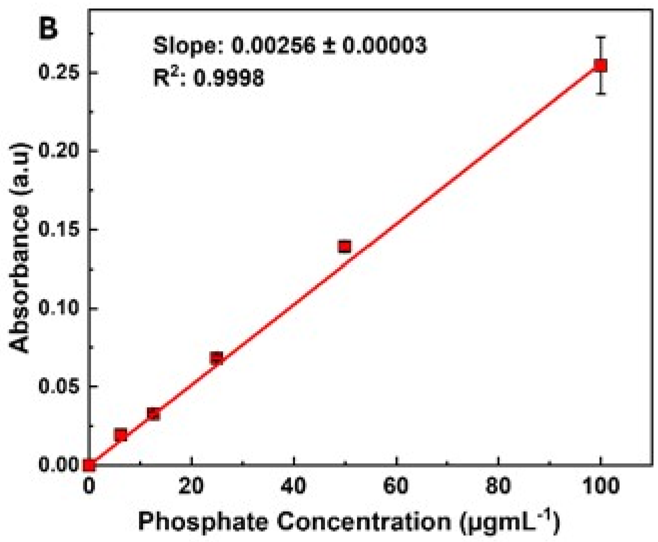

Figure S13. The calibration curve for free PO_4^{3-} determination.

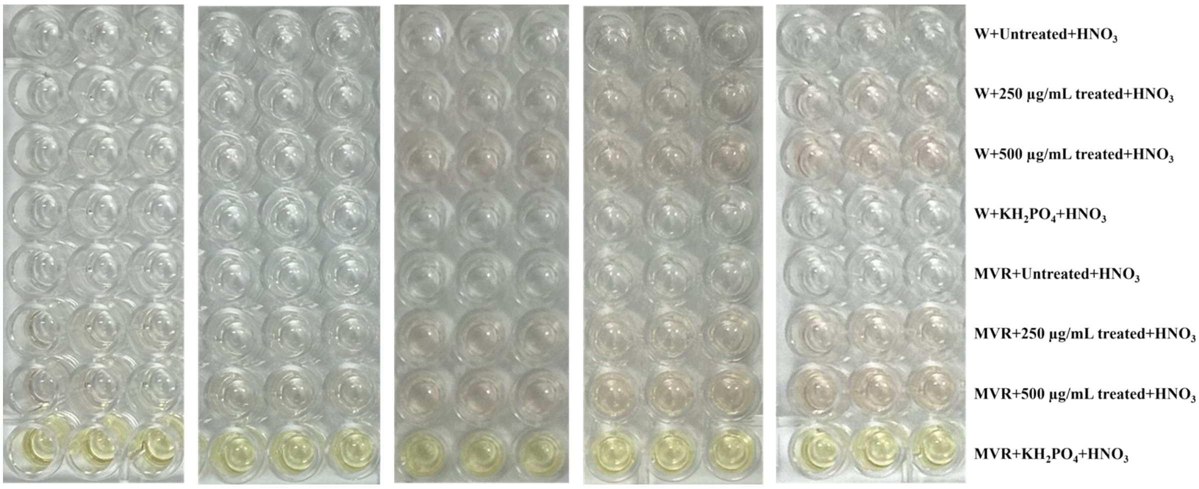

Figure S14. Free PO_4^{3-} determination.

Figure S15. Photogram of fresh bunch of tomatoes bought from the local supermarket.

DI Water

0 day

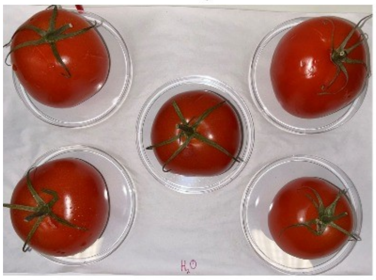

1 day

3 day

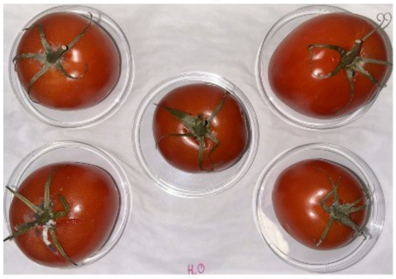

5 day

7 day

14 day

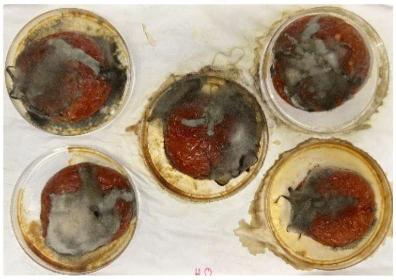

2.5 μg/mL

0 day

1 day

3 day

5 day

7 day

14 day

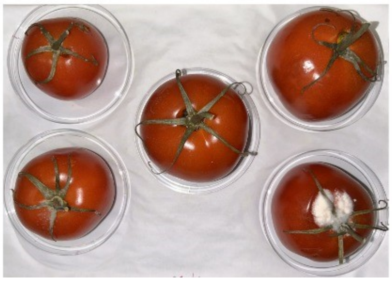

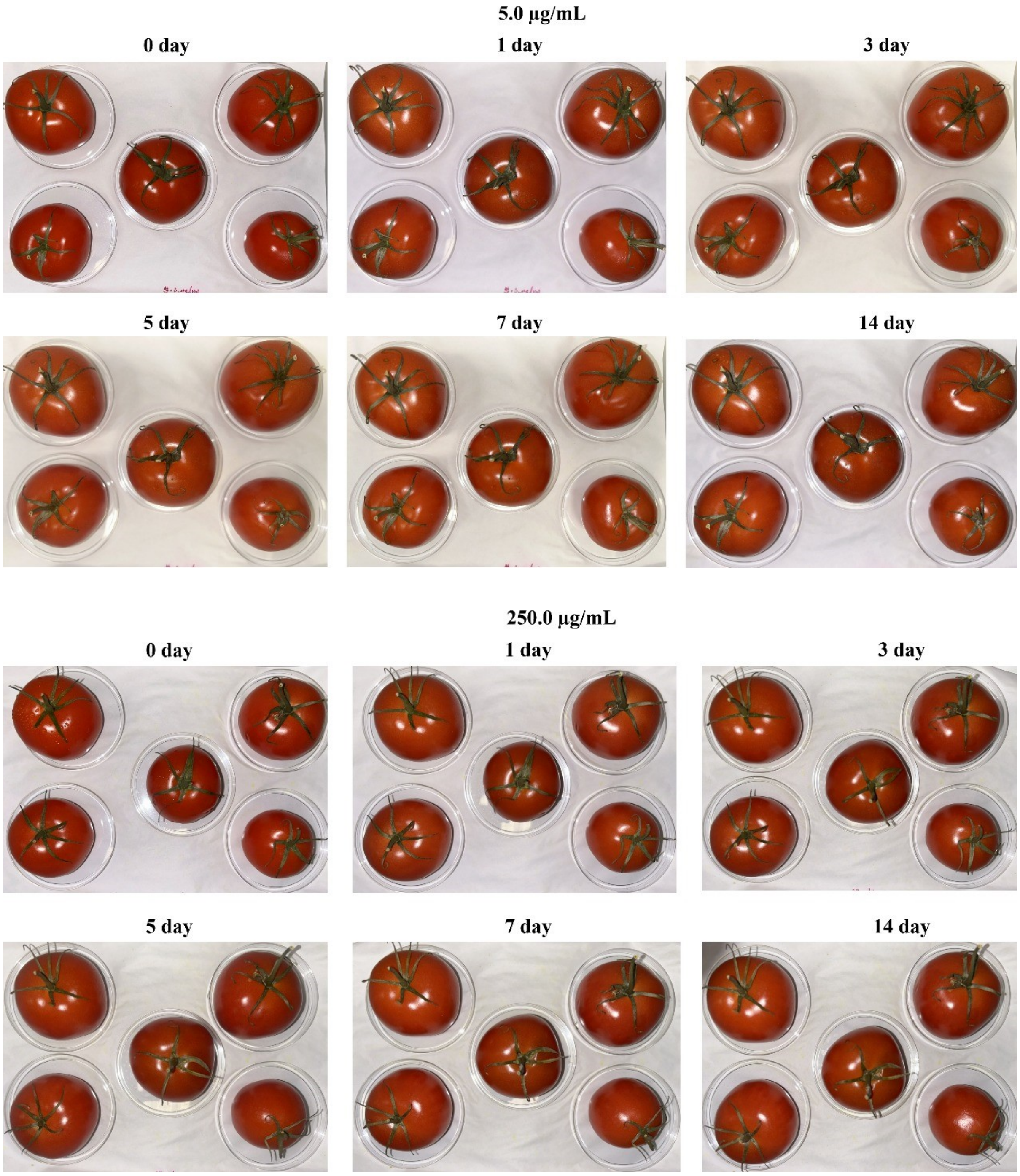

Figure S16. Preservation of tomatoes groups from molding with Cys-MR NPs at different concentrations by spraying. The spraying was done only on day 0. This experiment was done two times at room temperature in natural light (day/night) conditions.